Microtubule Dynamics and Chromosome Motion Visualized in Living Anaphase Cells

Gary J. Gorbsky, Paul J. Sammak, and Gary G. Borisy

Laboratory of Molecular Biology and Integrated Microscopy Resource for Biomedical Research, University of Wisconsin, Madison, Wisconsin 53706

Abstract. Chromosome segregation in most animal cells is brought about through two events: the movement of the chromosomes to the poles (anaphase A) and the movement of the poles away from each other (anaphase B). Essential to an understanding of the mechanism of mitosis is information on the relative movements of components of the spindle and identification of sites of subunit loss from shortening microtubules. Through use of tubulin derivatized with X-rhodamine, photobleaching, and digital imaging microscopy of living cells, we directly determined the relative movements of poles, chromosomes, and a marked domain on kinetochore fibers during anaphase. During chromosome movement and pole–pole separation, the marked domain did not move significantly with respect to the near pole. Therefore, the kinetochore microtubules were shortened by the loss of subunits at the kinetochore, although a small amount of subunit loss elsewhere was not excluded. In anaphase A, chromsomes moved on kinetochore microtubules that remained stationary with respect to the near pole. In anaphase B, the kinetochore fiber microtubules accompanied the near pole in its movement away from the opposite pole. These results eliminate models of anaphase in which microtubules are thought to be traction elements that are drawn to and depolymerized at the pole. Our results are compatible with models of anaphase in which the kinetochore fiber microtubules remain anchored at the pole and in which microtubule dynamics are centered at the kinetochore.

How kinetochore microtubules shorten in anaphase is a central question in the analysis of mitosis. In our previous effort to answer this question, we marked small domains on spindle fiber microtubules by photobleaching cells that had been microinjected with fluorescein-tubulin (Gorbsky et al., 1987). Phase-contrast observations of the living cell were followed by fixation and indirect immunofluorescence with an antibody to unbleached fluorescein, thus visualizing the photobleached domain as a region of reduced immunofluorescence. Each photobleached domain was then analyzed at a single time-point after photobleaching to determine its position with respect to the near pole during anaphase. We detected no significant movement and concluded that chromosomes move to the poles along stationary microtubules that shorten by loss of subunits at the kinetochore.

This conclusion runs counter to the generally accepted traction-fiber hypothesis, as expressed in recent textbooks (e.g., Alberts et al., 1983), that chromosomes are pulled toward opposite poles by forces that act on their kinetochore fibers, which get shorter and shorter by depolymerization at the pole. However, available evidence bearing on the site of depolymerization is indirect and contradictory. Forer's UV microbeam experiments (Forer, 1965) have generally been taken to indicate depolymerization at the pole, and Forer has reviewed and confirmed this interpretation (Forer, 1974, 1985). However, in other studies where he quantitated the changes in birefringence along the length of individual chromosomal fibers (Forer, 1976), he concluded the opposite—that fibers shorten through depolymerization at the kinetochore end.

Pickett-Heaps et al. (1982), on the basis of indirect evidence, have suggested that chromosomal fibers shorten at the kinetochore. Hiramoto and Shoji (1982) suggested that the force for chromosome motion is generated near the chromosomes, which is consistent with depolymerization at the kinetochore. However, in a photobleaching study from the same laboratory (Hamaguchi et al., 1987), it was reported that a bleached zone placed in the mitotic apparatus of a sand dollar egg moved poleward and, thus, that depolymerization of microtubules occurred at the pole. Mitchison et al. (1986), in a study using biotinylated tubulin, concluded that shortening occurred primarily by loss of subunits at the kinetochore, but that treadmilling and loss at the pole also took place at a lower rate. Finally, our analysis (Gorbsky et al., 1987) combining photobleaching and hapten-mediated immunocytochemistry pointed toward loss at the kinetochore. Clearly there is scope for further evaluation of this important question.

Given the methods of observation used in our previous

work, our analysis was limited to a single time-point per cell and conclusions were necessarily qualitative in nature. More definitive conclusions could be drawn from a quantitative, kinetic analysis of the relative movements of the components of mitotic spindles during anaphase in the living cell. This could be achieved by direct imaging of fluorescent tubulin. However, dichlorotriazinylamino-fluorescein–labeled tubulin, the derivative that has been used most commonly in previous studies on microtubule dynamics in vivo (Keith et al., 1981; Salmon et al., 1984; Saxton et al., 1984; Wadsworth and Salmon, 1986; Gorbsky et al., 1987; Hamaguchi et al., 1987; Sammak et al., 1987), photobleaches rapidly when living cells are observed by fluorescence microscopy. Furthermore, we noticed that mitotic cells microinjected with fluorescein-tubulin were sensitized to illumination with blue light and would fail to complete mitosis even after exposures of only a few seconds. In contrast, uninjected mitotic cells were unaffected by brief exposure to light from the mercury arc source.

To circumvent the problems encountered with fluorescein-tubulin, we have used a new derivative prepared by reaction of brain tubulin with the *N*-hydroxysuccinimide ester of x-rhodamine (Xrh).[1] This derivative, combined with the use of a highly sensitive video camera and digital imaging microscopy, has allowed us to visualize fluorescent microtubules in living cells at high resolution. Here, we extend our previous findings to a quantitative examination of the relative movements of chromosomes, mitotic poles, and kinetochore fiber microtubules during anaphase in living cells.

Materials and Methods

Protein Preparation

Microtubule protein was obtained from porcine brain by cycles of assembly and disassembly (Borisy et al., 1975). Pure tubulin was prepared from microtubule protein by DEAE-cellulose chromatography (Vallee and Borisy, 1978). Xrh-tubulin was prepared by reacting pure tubulin with carboxy-X-rhodamine-*N*-hydroxysuccinimide ester (Research Organics Inc., Cleveland, OH). Tubulin at 7–8 mg/ml was polymerized into microtubules at 37°C for 10 min in 0.1 M Pipes, 1 mM EGTA, 0.5 mM $MgCl_2$, 1 mM GTP, and 10% DMSO. The microtubules were sedimented at 20,000 *g* for 20 min at 37°C. The resulting pellet was resuspended in an ~20-fold volume of the same buffer without DMSO, and chilled at 0°C for 10 min to depolymerize the microtubules. This material was centrifuged at 20,000 *g* for 20 min at 0°C to eliminate any cold stable aggregates. DMSO to 10% was added to the supernatant (~4 mg/ml tubulin), and the material was warmed to 37°C to assemble microtubules. Carboxy-X-rhodamine-*N*-hydroxysuccinimide ester was dissolved at 10 mg/ml in DMSO. With rapid vortexing, the dye was added to the protein at a molar ratio of 60 to 1. After 15 min at 37°C, the reaction was quenched by adding a 10-fold molar excess of sodium glutamate. To remove assembly-incompetent tubulin and free dye, the microtubules were pelleted by centrifugation and subjected to two cycles of assembly and disassembly. Derivatized tubulin at 8 mg/ml was stored in small aliquots in liquid nitrogen. Yields were generally 30–50%. Based on an absorption coefficient of $6.3 \times 10^4\ M^{-1}\ cm^{-1}$ at 582 nm, the calculated dye-to-protein ratio of the conjugate varied from 0.2:1 to 0.4:1. For the experiments described here, a single preparation of derivatized tubulin with a dye-to-protein ratio of 0.4:1 was used throughout.

An in vitro–seeded assembly assay (Murphy et al., 1977) was used to test the effect on the polymerization of pure native tubulin when mixed with the Xrh derivative. At a final dye-to-tubulin ratio of 0.09:1, about the maximum expected in a microinjected cell, the mixture polymerized at 96% the initial rate and 87% the final extent of control, i.e., pure underivatized tubulin. Negative stain electron microscopy revealed that the mixed population assembled into primarily single microtubules with normal ultrastructure. Fluorescence microscopy of the same sample showed thin single fibers indicating that the derivative had been incorporated into the polymer (Sammak and Borisy, 1988).

1. *Abbreviation used in this paper*: Xrh, X-rhodamine.

Cell Culture and Microinjection

LLC-PK cells were grown in DME (Gibco, Grand Island, NY) supplemented with 10% FBS (HyClone Laboratories, Sterile Systems Inc., Logan, UT), 20 mM Hepes, and antibiotics. Cells were cultured in 35-mm dishes on glass coverslips containing carbon-finder patterns, and were microinjected in prophase or prometaphase as previously described (Gorbsky et al., 1987). After injection of several cells, the medium was replaced with MEM without phenol red, supplemented with 10% FBS, 20 mM Hepes, and antibiotics. This medium was prepared using a 100× stock of MEM amino acids and a 50× stock of MEM vitamins, also from Gibco. The medium in the culture dish was overlaid with mineral oil and the dish returned to the incubator to allow the cells to progress further into mitosis. After ~10 min in the incubator, culture dishes were transferred to the stage of the IM-35. The stage and culture dish were maintained at 34–35°C by means of an air curtain incubator (Nicholson Precision Instruments Inc., Gaithersburg, MD). A cell was allowed to enter anaphase and then photobleached.

Photobleaching

The photobleaching apparatus has been presented in detail previously (Gorbsky et al., 1987; Sammak et al., 1987) and is described briefly below. The 514.5-nm beam from an argon ion laser (model 2020, Spectra-Physics Inc., Mountain View, CA) was imaged through a 300-mm focal length lens and a 200-mm focal length cylindrical lens to produce a bar-shaped beam focused in the specimen plane. The laser was operated at 400–600 mW with an exposure of 500 ms, and the beam was attenuated by a 0.9 OD neutral density filter. The beam was channeled into the epiillumination system of an inverted microscope (model IM-35, Carl Zeiss Inc., Thornwood, NY). When focused through a planapochromat 100×, 1.3 N.A. objective, the beam produced a bleached band ~2 μm wide in the spindle of a typical injected cell.

Immunolabeling

A few anaphase cells and some interphase cells were prepared for immunolabeling with antitubulin to ascertain whether photobleaching had damaged microtubules. Within a short time of photobleaching (a few seconds for anaphase cells and a few minutes for interphase cells), coverslips were twice rinsed in a buffer containing 60 mM Pipes, 25 mM Hepes, 10 mM EGTA, and 2 mM $MgCl_2$, pH 6.95. The cells were then lysed with 0.5% Triton X-100 in the same buffer for 90 s. Then the cells were fixed for 20 min in 5 mM ethylene glycol bissuccinic acid *N*-hydroxysuccinimide ester (Sigma Chemical Co., St. Louis, MO). The fixative was prepared as a 100-mM stock in DMSO. Just before use, 100 μl of the stock was added to 1.9 ml of buffer.

After fixation, the cells were rinsed several times with 140 mM NaCl, 3 mM KCl, 10 mM PO_4, 3 mM NaN_3, pH 7.3 (PBS), and processed for immunolabeling with antitubulin and a fluorescein secondary antibody as described previously (Gorbsky et al., 1987).

Imaging of Living Cells

Phase and fluorescent images of living cells were visualized with a silicon-intensified target video camera (model 66; DAGE-MTI, Wabash, MI). A tungsten light source provided illumination for phase-contrast microscopy, while a 100-W point mercury arc source served for fluorescence excitation. The mercury arc light was attenuated by neutral density filters of OD 0.3–1.2, depending on the intensity of the fluorescent spindle and the age of the mercury arc light bulb.

Images from the camera were processed with an image processor (model 9200; Quantex Corp., Sunnyvale, CA) and recorded with a high resolution 3/4-inch video tape recorder (model NV9240XD; Panasonic Co., Secaucus, NJ). Phase images were processed by averaging 16 or 32 video frames to minimize noise from the camera. Fluorescent images were processed in two ways. For focusing, averaged images of three video frames (0.1-s total exposure) were captured in the processor image memory and displayed on the video monitor. When the correct focal plane had been found, images of higher quality were recorded by summing 16–75 video frames (0.5–2.5-s total exposure). Automatic sequences for the opening and closing of shutters (Vincent Associates, Rochester, NY) and the capture of images into the processor memories were controlled by programs from the processor. Fluo-

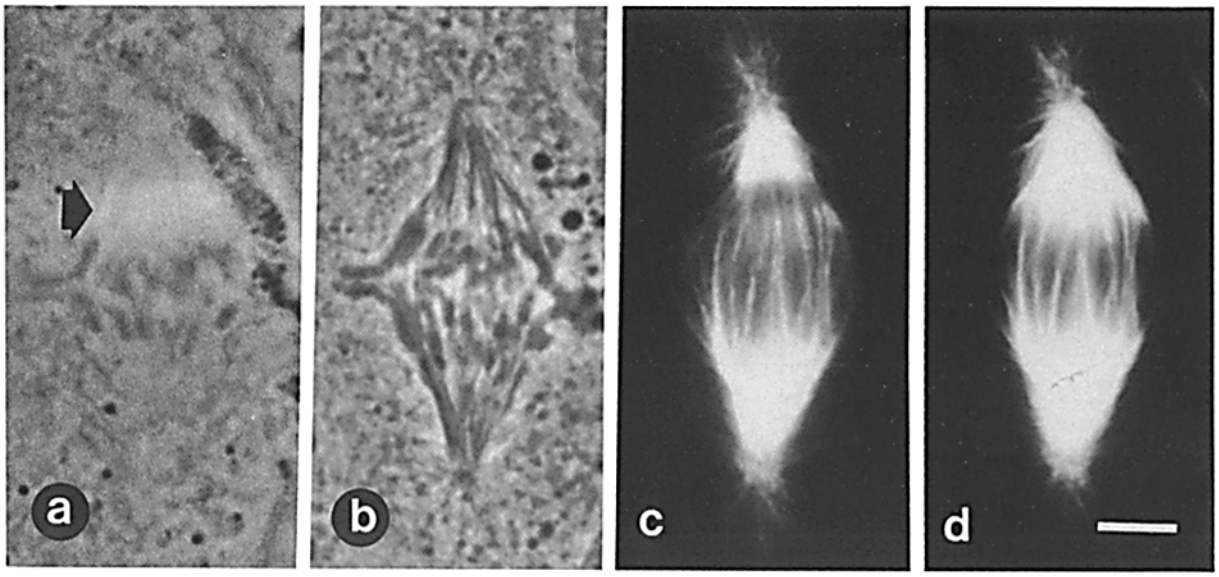

Figure 1. Photobleaching does not disrupt microtubule bundles. (*a*) Phase-contrast image of living cell at moment of photobleaching with superimposed exposure of light emitted from Xrh-tubulin upon excitation by laser (*arrow*). (*b*) Phase-contrast image of same cell lysed and fixed 25 s after photobleaching. (*c*) Fluorescence image of Xrh emission from lysed cell. (*d*) Antitubulin immunofluorescence. The Xrh fluorescence shows a distinct bleached zone. The antitubulin immunofluorescence reveals that fibers are present and continuous through the bleached zone. Bar, 5 μm.

rescent images recorded on video tape were optimized to enhance contrast by adjusting image gain and offset with the image processor. The images were displayed on a high-resolution black and white monitor (Sierra Scientific Corp., Mountain View, CA), photographed with 35-mm Tech Pan 2415 film, and developed with HC-110, dilution F.

Data Analysis

Digital images of the living cells were used to quantitate the positions of poles, chromosomes, and bleached zones. The following procedure was used to achieve a consistent means of locating spindle poles. A fluorescent image of a spindle was displayed on the video monitor and a line defining the spindle axis was entered into the overlay memory. A cursor was then positioned on the line and radiance measurements were taken to determine the brightest position in a pole vicinity. The abequatorial pixel position at 80% maximum brightness was arbitrarily chosen to define the pole. The position of the bleached zone on a fluorescence image was defined as the center of the bleached area intersecting the spindle axis.

The average chromosome-to-pole distances were determined as follows. The positions of the poles, determined as described above for the fluorescent image nearest in time, were marked on the phase image of the spindle. Next, an acetate overlay containing 11 parallel lines was placed over the image such that the central line connected the two poles (spindle axis). A line perpendicular to the spindle axis was then drawn through each pole (pole horizontal). The positions of the chromosomes were determined as the most poleward points where they intersected each of the 11 lines. Distances between the chromosomes and the pole horizontal were computed and the chromosome-to-pole distance was calculated as the mean of the 11 measurements. To obtain the correct radial distance from the pole, these measurements should be divided by the cosine of the angle subtended by each kinetochore fiber on the spindle axis. However, because microscopy allows only a two-dimensional image of a three-dimensional structure, and because the chromosomes and kinetochore fibers overlapped, it was not possible to determine this angle for each chromosome. Nevertheless, the error in neglecting radial correction was not great. Assuming that on average a chromosome lay 25 degrees off the spindle axis, the true distance would be underestimated by 10%.

Results

Experimental Design

Our experimental plan was to create a reference mark on kinetochore microtubules by photobleaching a domain in the half-spindle after the cell had equilibrated with fluorescently labeled tubulin. Xrh-tubulin microinjected into cells incorporated normally into the spindle microtubules and had no apparent effect on the progress of cells through mitosis. In contrast with fluorescein-tubulin, several fluorescent images of cells microinjected with Xrh-tubulin could be obtained without appreciably bleaching the fluorescence of the microtubules or disturbing mitosis. However, the amount of mercury arc illumination that could be tolerated was still limited. For this reason we kept exposures short, attenuated the mercury arc light source with neutral density filters, and took only five or fewer images of each cell.

Previous investigators have reported that illumination of sufficient intensity to cause photobleaching in a cell microinjected with fluorescein-tubulin does not cause ultrastructural damage to the illuminated microtubules (Saxton et al., 1984; Keith, 1987). Because Xrh is more resistant to photobleaching, it was necessary to use higher intensities of laser light than were used in our previous studies with fluorescein-tubulin. To verify that the laser photobleaching did not cause disorganization of kinetochore fiber bundles, we lysed and fixed cells soon after photobleaching and processed them for antitubulin immunofluorescence (Fig. 1). When visualized for Xrh emission, clear bleached zones were seen in the spindles. The antitubulin immunofluorescence showed that no disruption of the kinetochore fibers was apparent. In interphase cells, where individual microtubules could be more easily distinguished, no breakage of the microtubules after photobleaching could be detected (data not shown).

Analysis of Individual Cells

Fig. 2 shows a photobleaching experiment in a cell that was injected in prophase with Xrh-tubulin. Fig. 2 *a* was taken 42 s after anaphase onset but before photobleaching. The cell was photobleached at 60 s and the image in Fig. 2 *b* was

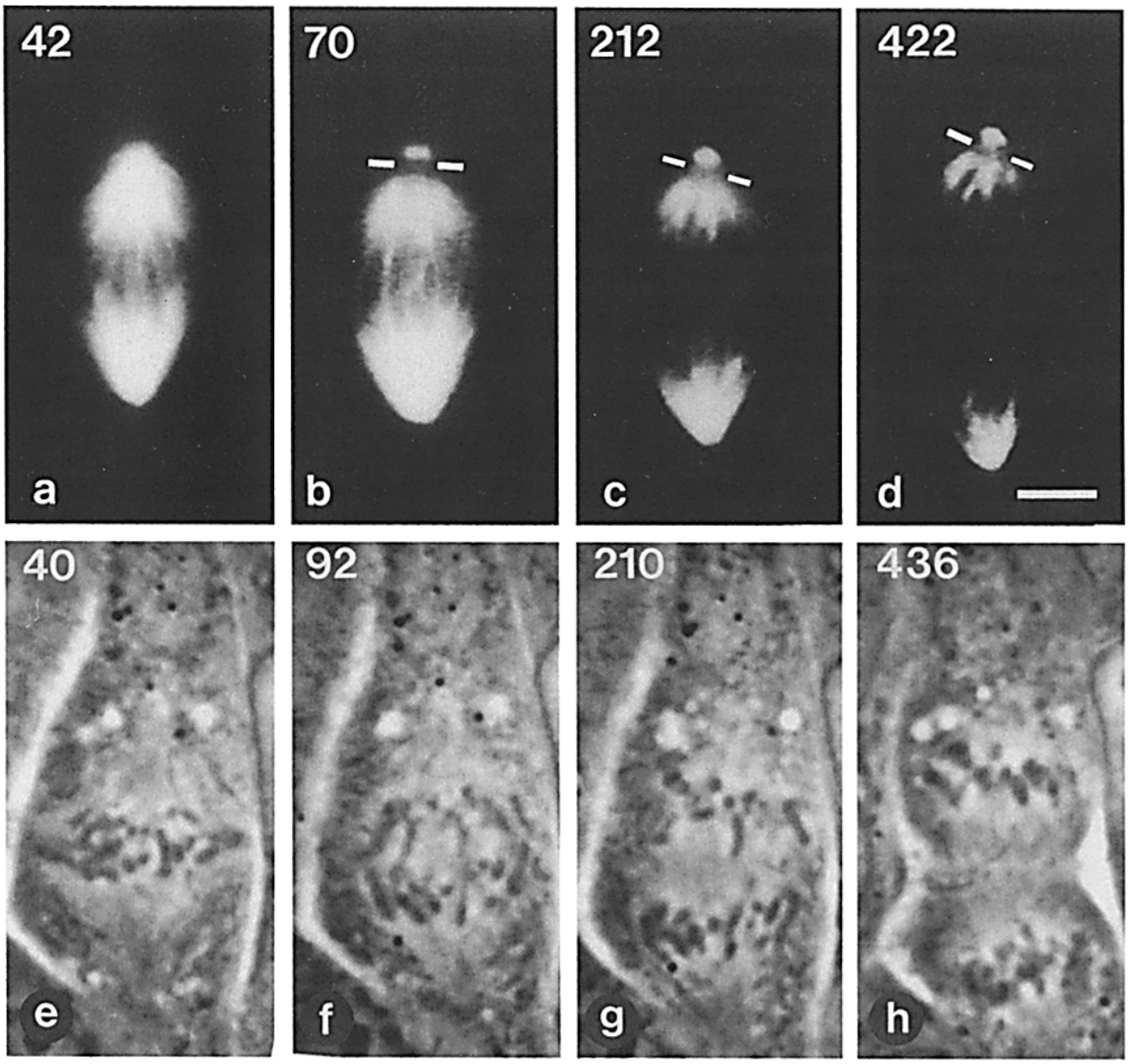

Figure 2. Photobleaching experiment in living anaphase cell. (*a*) Fluorescence and (*e*) phase-contrast images of early anaphase cell before photobleaching. The cell was photobleached at 60 s. (*b–d*) Fluorescence and (*f–h*) phase-contrast images demonstrating the progression of the cell after photobleaching. The bleached zone (*bars*) remained stationary with respect to the near pole as the kinetochore fibers shortened. The bleached zone also accompanied the pole in its migration away from the spindle equator. As sometimes happens, the spindle underwent a twisting motion in late anaphase. Time in seconds after anaphase onset is indicated in the upper lefthand corner of each panel. Bar, 5 μm.

captured at 70 s. The bleached zone appeared as a dark band ~2 μm wide, 2 μm from the upper pole. In Fig. 2 *c*, taken 212 s after anaphase onset, the cell had progressed in anaphase and the bleached zone, although less distinct, remained clearly visible. Yet later, 422 s after anaphase onset (Fig. 2 *d*), when chromosome movement had almost ceased and the cell had begun to cleave, the bleached zone, though less distinct, was still apparent. The phase-contrast images (Fig. 2, *e–h*) show the positions of the chromosomes at various times during the process. During the extensive anaphase motion of the chromosomes, the bleached zone did not move appreciably with respect to the near pole although the poles separated considerably. In Fig. 3 the movements of the poles, bleached zone, and average leading position of the chromosomes are quantitated for the cell shown in Fig. 2. While the chromosomes approached the bleached zone, the zone itself did not move appreciably with respect to the near pole. However, the bleached zone did move with respect to the spindle equator accompanying the outward motion of the pole.

If it is true that kinetochore fiber microtubules do not move toward the pole during the time that they are shortening in anaphase, then a bleached zone placed closer to the chromosomes in early anaphase should be encroached upon and finally overrun by the advancing chromosomes. Such an experiment is exemplified by Fig. 4. Fig. 4 *a* shows the cell 26 s after anaphase onset and 10 s after photobleaching. The positions of the chromosomes at 24 s after anaphase onset are seen in Fig. 4 *d*. By 96 s (Fig. 4 *b*), the bleached zone has been encroached upon by the advancing chromosomes which are shown at 94 s in Fig. 4 *e*. Finally by 260 s (Fig. 4 *c*),

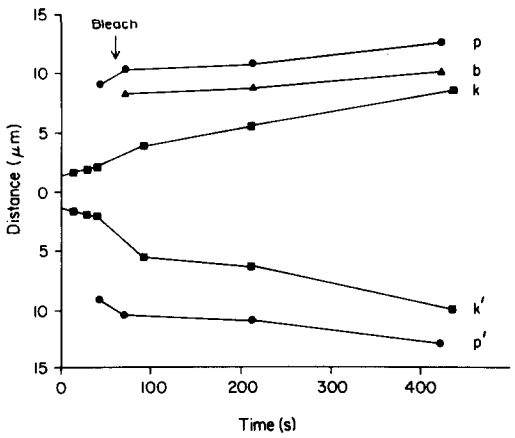

Figure 3. Movements of spindle components. Data for the cell pictured in Fig. 2 are plotted with respect to the equator (defined as the midpoint between the poles). From the moment of photobleaching (*arrow*), the kinetochore (*k*)-to-pole (*p*) distance decreased by 2.9 μm, while the bleached zone (*b*)-to-pole distance changed only slightly (apparent increase of 0.4 μm). Time zero is the onset of anaphase. *k'*, Average position of kinetochores in lower half-spindle; *p'*, lower pole.

the bleached zone has disappeared, overrun by the chromosomes shown at 232 s in Fig. 4 *f*.

Cumulative Results

A total of 29 cells were photobleached in anaphase. All completed anaphase. Of these, 2 were not observed past anaphase, 3 failed to cleave, and the remaining 24 completed cytokinesis normally. 4 of the 29 cells were photobleached twice, once in each half spindle. All 4 cleaved normally. In three cases, such as that shown in Fig. 4, the bleached zones were encroached upon or overrun by the chromosomes at the time that the second fluorescent image after photobleaching was taken. These bleaches were excluded from the quantitative analysis described below.

The separation of the poles (anaphase B) was variable from cell to cell and seemed to be correlated to some extent with cell morphology. Long narrow cells tended to exhibit greater pole separation than did the more squat cells. The largest extent of pole movement seen was 5.4 μm. The rate of pole migration appeared to be similarly related to cell morphology averaging 0.6 ± 0.4 μm/min (mean ± SD). Some of the measured variation in the extent and rate of pole separation may also be due to the fact that all cells were not analyzed for precisely the same time interval during anaphase.

In Fig. 5 we compare the movements of the poles with the movements of the bleached zones away from the spindle equator. The two movements were closely related showing a slope of 1.04 ± 0.06 (estimated standard error of the slope) by least squares analysis and a correlation coefficient of 0.97. This result indicates that the bleached zones accompanied the poles in their movements away from the equator. Thus, the kinetochore fiber microtubules of the half-spindle accompany the near pole during pole–pole separation.

After determining the contribution of anaphase B, we were then in a position to analyze anaphase A. To combine data from all the cells in comparing the relative movement of bleached zones, chromosomes, and poles, we calculated rates of movement of chromosomes and bleached zones with respect to their near poles (Fig. 6). The average rate of chromosome movement was 0.95 ± 0.44 μm/min (mean ± SD). However, the rate of chromosome motion varied with time in any given cell. Initially, chromosomes separated slowly, then accelerated to their most rapid rate in mid-anaphase, and finally slowed down as they neared the pole in late anaphase. For most of the cells studied, only the most rapid phase of chromosome motion was recorded. However, some cells were observed into late anaphase, when the chromosomes had slowed considerably. The 10 cells observed for the longest times after anaphase onset are shaded in Fig. 6 *A*. Excluding those 10 cells the rate of chromosome motion was 1.12 ± 0.44 μm/min. In contrast to the rapid movement of the chromosomes, the bleached zones showed an apparent average rate of movement of only 0.095 ± 0.13 μm/min toward the pole. With the exclusion of the 10 late anaphase cells, this figure was 0.10 ± 0.14 μm/min. These results indicate that the majority of the kinetochore fiber microtubules moved little, if at all, with respect to the pole during anaphase, and that all or nearly all of the movement of the chromosomes toward the pole was accountable by shortening of microtubules at the kinetochore.

While the mean rate of movement of bleached zones toward the pole was not significantly different from zero, a few cells exhibited relatively greater rates of movement. The source of this variation is unknown. In any case, our results demonstrate that at most 10% of anaphase A chromosome movement and depolymerization of kinetochore fiber microtubules could be brought about by movement of the microtubules with respect to the pole, or by their disassembly at a location other than the kinetochore.

Discussion

Microtubule Dynamics in Living Anaphase Cells

We have investigated the relative motions of chromosomes, their kinetochore microtubules, and the mitotic poles in anaphase by recording fluorescent images from living cells photobleached after microinjection with a new tubulin derivative. Unlike most previous observations of fluorescently derivatized tubulin within living cells (Salmon et al., 1984; Saxton et al., 1984; Wadsworth and Salmon, 1986; Hamaguchi et al., 1987), a different fluorophore (Xrh vs. fluorescein) and a different linking chemistry (the *N*-hydroxysuccinimide ester vs. the dichlorotriazinylamino group) were used. The fluorescein and Xrh derivatives behaved indistinguishably within the cell, lending support to the idea that microinjection of tracer amounts of derivatized tubulin does not perturb cellular processes. In the present study, quantitative data about the relative motions of spindle components were obtained by fluorescence imaging of living cells through the use of a highly sensitive video camera and digital image processing.

We interpret our fluorescent images as visualizing primarily pole-to-kinetochore microtubules. In the LLC-PK cell line, these microtubules are gathered into dense bundles that comprise the bulk of the fluorescence in immunofluorescently stained specimens (Gorbsky et al., 1987). In our images of the living cells, astral microtubules were not evident

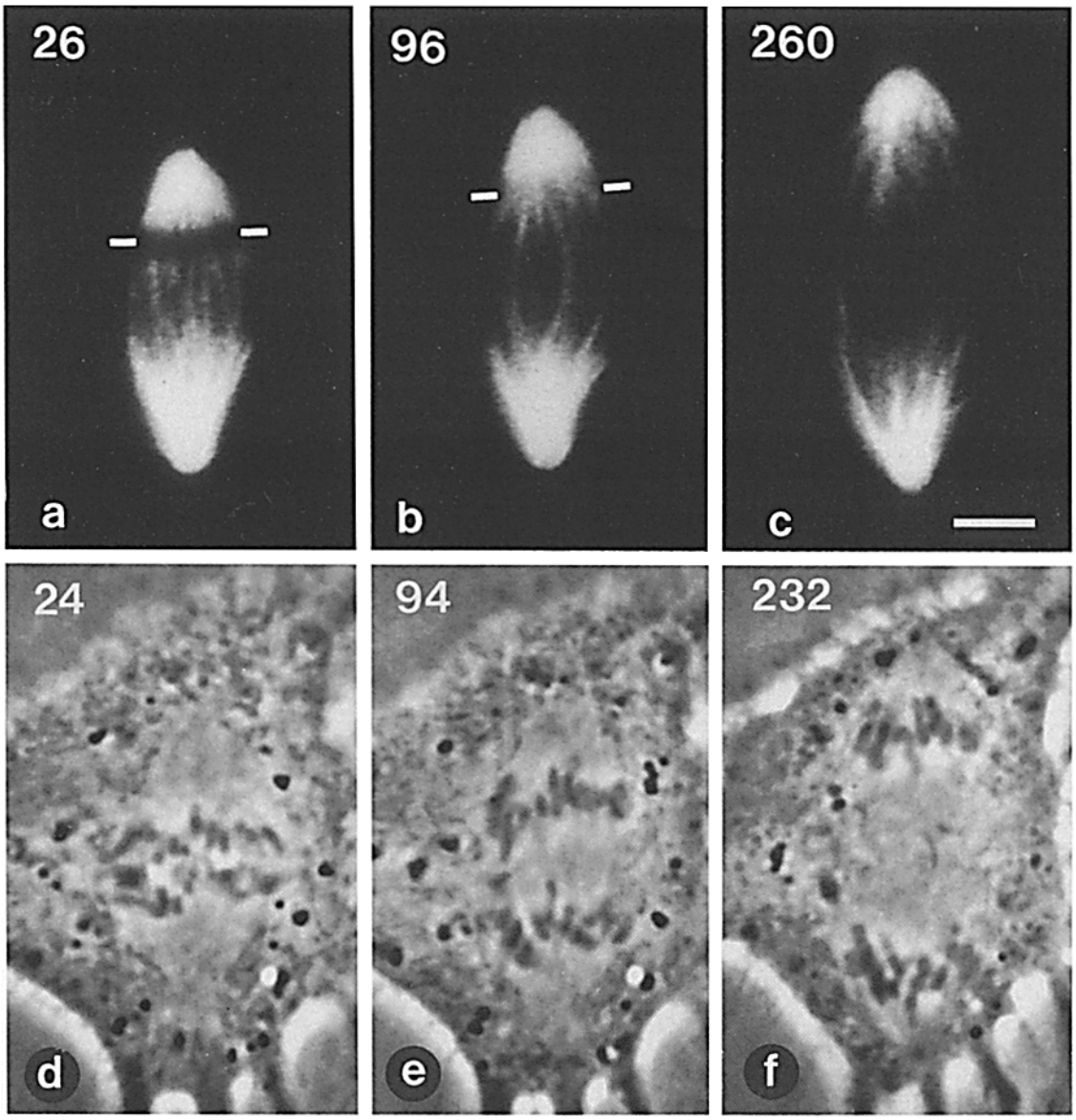

Figure 4. Photobleaching experiment in living anaphase cell demonstrating encroachment and overrunning of the bleached zone by the chromosomes. (*a–c*) Fluorescence and (*d–f*) phase-contrast images showing progression of anaphase in cell photobleached at 16 s after anaphase onset. In *a*, the bleached zone is just ahead of the advancing chromosomes. By the time that *b* was taken, the chromosomes had partially encroached rendering the bleached zone (*arrow*) less distinct. By 260 s (*c*), the bleached zone had been overrun by the chromosomes. Bar, 5 μm.

above background, and few fluorescent microtubule bundles were detectable in the interzonal region between the separating chromosomes. Throughout mitosis, pole-to-chromosome fibers could be easily distinguished from interzonal bundles. Thus, our bleached zones represented a reduction in fluorescence primarily in these pole-to-chromosome microtubule bundles.

Generally, bleached zones in the spindles of living cells became somewhat less distinct as anaphase progressed. Several factors probably account for this observation. First, the spindle changes shape during anaphase causing the kinetochore fibers to shift slightly, relative to each other. This shifting causes the borders of the bleached domains to become misaligned. Second, some recovery of the fluorescence within the area of the bleached zone takes place. The detailed mechanism of fluorescence redistribution remains to be established, but it probably involves turnover of some of the spindle microtubules. During anaphase, the astral microtubules elongate and interzonal bundles become more prominent. The turnover and assembly of these microtubules, incorporating fluorescent tubulin in the region of the bleached zone, would result in a decreased contrast of the bleached zone. The recruitment of interzonal fiber microtubules into bleached zones of the spindle was detected directly in our previous study of anaphase in which cells were lysed and fixed and then labeled with antifluorescein antibodies (see Figs. 3 and 4 in Gorbsky et al., 1987).

If significant numbers of kinetochore fiber microtubules were drawn to the poles in anaphase, then large bundles of fluorescence should invade the bleached zone. Such an inva-

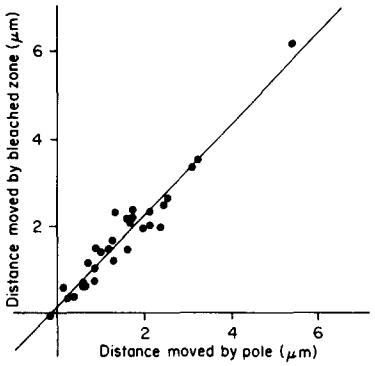

Figure 5. The bleached zone moves together with the pole in anaphase B. The movement of each bleached zone (with respect to the midpoint between the poles) is plotted vs. the movement of its associated pole. Although the magnitude of anaphase B was variable, linear least squares regression analysis showed that bleached zone movement was proportional to pole movement. Slope, 1.04 ± 0.06 (estimated standard error of the slope); intercept, 0.16 ± 0.11 (estimated standard error of the intercept); correlation coefficient, 0.97.

sion was not observed. We cannot at present eliminate the possibility that one or a very few kinetochore microtubules had translocated through the bleached zones. However, we feel it unlikely that one or a very few poleward moving kinetochore fiber microtubules are entirely responsible for chromosome movement. Complete accounting of microtubule dynamics within the anaphase spindle requires analysis of photobleaching experiments at the ultrastructural level. We are currently pursuing such studies.

The fact that bleached zones generally remained stationary in anaphase strongly suggested that the kinetochore fibers remained stationary with respect to the near pole. Significant movement of a bleached zone toward the pole was detected only rarely; thus we feel that translocation of kinetochore microtubules toward the pole is not a requisite event in anaphase and contributes only marginally, if at all, to chromosome movement. One explanation of why a few cells exhibited greater than usual amounts of bleached zone movement toward the pole is as follows. Cells showed varying amounts of changes in the shapes of their spindles during progression through anaphase. The mitotic spindle is a three-dimensional structure. Shape changes may artificially distort our two-dimensional images and our one-dimensional measurements. For example, the spreading away from one another of the kinetochore fibers late in anaphase as the chromosomes crowd in toward the pole would result in an apparent movement of a bleached zone toward the pole.

Our results with the living cells extend the findings of our previous study in which cells were analyzed by hapten-mediated immunocytochemistry after photobleaching. In both sets of experiments a photobleached zone was used to mark a domain on kinetochore microtubules. In the hapten-mediated immunocytochemical study, we were limited to one time-point per cell, but with direct imaging used here we obtained multiple data points on the same cell, which permitted kinetic analysis.

The kinetic analysis demonstrated that, for pole–pole separation (anaphase B), the kinetochore fiber microtubules accompanied the near pole in its movement away from the spindle equator. During the movement of the chromosomes to the pole (anaphase A), the kinetochore microtubules remained essentially stationary with respect to the near pole. Bleached domains placed near the kinetochore in an early anaphase cell were approached, invaded, and subsequently overrun by the advancing chromosomes, indicating that kinetochore fiber microtubules dissassemble at the kinetochore during anaphase. Thus the chromosomes move to the pole by translocating along kinetochore-to-pole microtubules.

Similar conclusions were reached by Mitchison et al. (1986), who used electron microscopic immunocytochemistry to follow the incorporation of biotin-tubulin into metaphase cells. When cells were fixed at very short times after microinjection, they found that tubulin had been incorporated into the kinetochore fiber microtubules at the kinetochore. With longer intervals between injection and fixation, the label in the kinetochore fiber microtubules incorporated progressively toward the pole. The authors interpreted these experiments to indicate the existence of a poleward treadmilling of microtubule subunits from the kinetochore to the pole at an average rate of 0.5 μm/min. They suggested that this flux continues in anaphase. However, because cells injected in metaphase which rapidly entered anaphase showed little or no label at their kinetochores, the authors also concluded

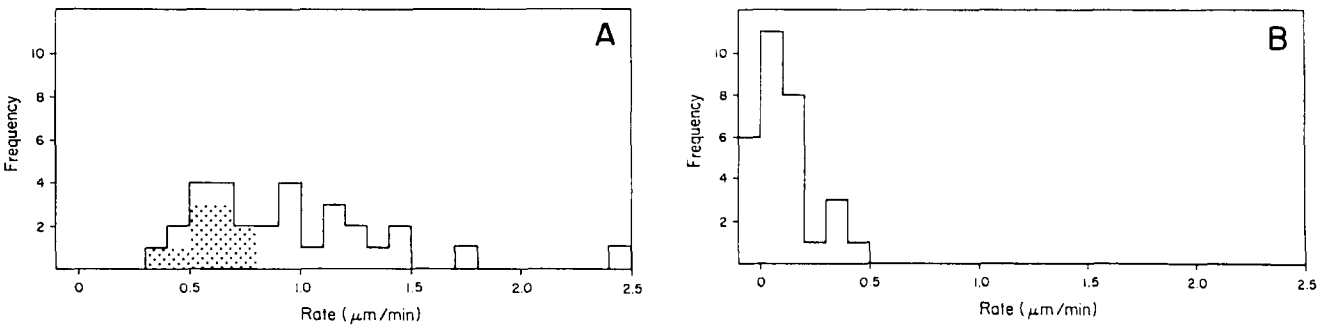

Figure 6. Quantitative analysis of anaphase A. Rates of movement of the chromosomes (*A*) are compared to rates of movement of the bleached zones (*B*) for all photobleaching experiments. The rates were normalized by subtracting the movements of bleached zones and chromosomes due to pole-pole separation. The average rate of movement for the bleached zones was 0.095 ± 0.13 μm/min (mean ± SD) toward the pole. The average rate for the chromosomes was 0.95 ± 0.44 μm/min (mean ± SD). 10 cells (*shaded bars in A*) were observed in late anaphase, when chromosome motion had slowed considerably, thus lowering their overall average rates of chromosome movement (see text).

that most loss of microtubule subunits during anaphase occurs at the kinetochore.

Our quantitative analysis of living cells permits us to place an upper limit on possible movement of the bleached zone with respect to the pole during anaphase. Most cells showed no significant movement. Some showed slight movement of the bleached zone toward the pole, and a few showed slight movement away from the pole. Movement of the bleached zone toward (or away from) the pole would be predicted if a small amount of depolymerization (or polymerization) of kinetochore fiber microtubules occurred at locations other than the kinetochore; e.g., at the pole or along the length of the fiber. On the other hand, the apparent movement of a bleached zone toward or away from the pole may be due to other factors, such as shape changes in the spindle during anaphase. Our data did not allow us to distinguish among these possibilities; however, such movement could account for, at most, only 10% of the movement of the chromosomes and 10% of the disassembly of the kinetochore fiber microtubules. Our results indicate that at least 90% of the chromosome's motion comes about through the loss of microtubule subunits at the kinetochore.

In conclusion, our results indicate that during anaphase the kinetochore fiber microtubules are anchored at the pole and accompany the pole in its anaphase B motion. For anaphase A, the predominant site of microtubule disassembly is at the kinetochore.

We thank John Peloquin and Bohdan Soltys for advice and help in the preparation of derivatized proteins; Steve Limbach and Leslie Rabas for illustration; and Patricia Hanson for manuscript preparation. We also thank Hans Ris and Gerald Schatten for critical reading of the manuscript.

This work was supported by National Institutes of Health grants GM25062 to Gary G. Borisy and RR00570 to the Integrated Microscopy Resource for Biomedical Research at the University of Wisconsin at Madison.

Received for publication 25 September 1987, and in revised form 18 December 1987.

References

Alberts, B., D. Bray, J. Lewis, M. Raff, K. Roberts, and J. D. Watson. 1983. Molecular Biology of the Cell. Garland Publishing Inc., New York. 656–658.

Borisy, G. G., J. M. Marcum, J. B. Olmsted, D. B. Murphy, and K. A. Johnson. 1975. Purification of tubulin and associated high molecular weight proteins from porcine brain and characterization of microtubule assembly *in vitro*. *Ann. N.Y. Acad. Sci.* 253:107–132.

Forer, A. 1965. Local reduction of spindle fiber birefringence in living *Nephrotoma suturalis* (Loew) spermatocytes induced by ultraviolet microbeam irradiation. *J. Cell Biol.* 25(Suppl.):95–117.

Forer, A. 1974. Possible roles of microtubules and actin-like filaments during cell-division. *In* Cell Cycle Controls. G. M. Padilla, I. L. Cameron, and A. M. Zimmerman, editors. Academic Press Inc., New York. 319–336.

Forer, A. 1976. Actin filaments and birefringent spindle fibers during chromosome movements. *In* Cell Motility. R. Goldman, T. Pollard, and J. Rosenbaum, editors. Cold Spring Harbor Laboratory, Cold Spring Harbor, New York. 1–28.

Forer, A. 1985. Does actin produce the force that moves a chromosome to the pole during anaphase? *Can. J. Biochem. Cell Biol.* 63:585–598.

Gorbsky, G. J., P. J. Sammak, and G. G. Borisy. 1987. Chromosomes move poleward in anaphase along stationary microtubules that coordinately disassemble from their kinetochore ends. *J. Cell Biol.* 104:9–18.

Hamaguchi, Y., M. Toriyama, H. Sakai, and Y. Hiramoto. 1987. Redistribution of fluorescently labeled tubulin in the mitotic apparatus of sand dollar eggs and the effect of taxol. *Cell Struct. Funct.* 12:43–52.

Hiramoto, Y., and Y. Shoji. 1982. Location of the motive force for chromosome movement in sand dollar eggs. *In* Biological Functions of Microtubules and Related Structures. H. Sakai, H. Mohri, and G. G. Borisy, editors. Academic Press Inc., New York. 247–259.

Keith, C. H. 1987. Slow transport of tubulin in the neurites of differentiated PC12 cells. *Science (Wash. DC)*. 235:337–339.

Keith, C. H., J. R. Feramisco, and M. Shelanski. 1981. Direct visualization of fluorescein-labeled microtubules *in vitro* and in microinjected fibroblasts. *J. Cell Biol.* 88:234–240.

Mitchison, T., L. Evans, E. Schulze, and M. Kirschner. 1986. Sites of microtubule assembly and disassembly in the mitotic spindle. *Cell.* 45:515–527.

Murphy, D. B., K. A. Johnson, and G. G. Borisy. 1977. Role of tubulin-associated proteins in microtubule nucleation and elongation. *J. Mol. Biol.* 117:33–52.

Pickett-Heaps, J. D., D. H. Tippit, and K. R. Porter. 1982. Rethinking mitosis. *Cell.* 29:729–744.

Salmon, E. D., R. J. Leslie, W. M. Saxton, M. L. Karow, and J. R. McIntosh. 1984. Spindle microtubule dynamics in sea urchin embryos: analysis using a fluorescein-labeled tubulin and measurements of fluorescence redistribution after laser photobleaching. *J. Cell Biol.* 99:2165–2174.

Sammak, P. J., and G. G. Borisy. 1988. Detection of single fluorescent microtubules and methods for determining their dynamics in living cells. *Cell Motil. Cytoskeleton.* In press.

Sammak, P. J., G. J. Gorbsky, and G. G. Borisy. 1987. Microtubule dynamics in vivo: a test of mechanisms of turnover. *J. Cell Biol.* 104:395–405.

Saxton, W. M., D. L. Stemple, R. J. Leslie, E. D. Salmon, M. Zavortnik, and J. R. McIntosh. 1984. Tubulin dynamics in cultured mammalian cells. *J. Cell Biol.* 99:2175–2186.

Vallee, R. B., and G. G. Borisy. 1978. The non-tubulin component of microtubule protein oligomers. *J. Biol. Chem.* 253:2834–2845.

Wadsworth, P., and E. D. Salmon. 1986. Analysis of the treadmilling model during metaphase of mitosis using fluorescence redistribution after photobleaching. *J. Cell Biol.* 102:1032–1038.